ELSEVIER

Journal of Organometallic Chemistry 563 (1998) 95–99

Journal of Organo metallic Chemistry

Formation of a strained [3]ferrocenophane via base-catalyzed intramolecular cyclization

Chi-Fa Chiu, Chien-Liang Hwang, Dung-Shien Pan, Yuan Jang Chen, Keh Shin Kwan *

Department of Chemistry Fu Jen University, Taipei, Taiwan

Received 16 January 1998; received in revised form 17 March 1998

Abstract

Synthesis of 1,3-diferrocenyl-3-methyl[3]ferrocenophan-1-ene by base-catalyzed intramolecular cyclization is described. The molecular structure of the title compound has been determined by single-crystal X-ray analysis. It crystallizes in monoclinic space group $P2_1/c$ with $a = 15.580(6)$ Å, $b = 9.512(3)$ Å, $c = 34.493(9)$ Å, $\beta = 98.20(3)°$, $Z = 8$, and $V = 5060(3)$ Å^3. © 1998 Elsevier Science S.A. All rights reserved.

Keywords: Intramolecular cyclization; [3]ferrocenophane; Crystal structure

---

1. Introduction

Considerable research effort has been devoted to the study of ferrocenophanes, in particular, [*m*]ferrocenophanes by Watts et al. [1–3], [*m.n*]ferrocenophanes and [*m*]^{n}ferrocenophanes by Westerhoff et al. [4–6]. As indicated in literature, the most commonly used routes to synthesize [3]ferrocenophanes are acid-catalyzed intramolecular acylation of β-ferrocenylpropionic acids to the corresponding bridged ketones, and base-catalyzed intramolecular cyclization reactions are rare [1].

Our intention to study mixed-valence chemistry in the following compound **A** and the hypothetical compound **B** leads us to synthesize its precursor compound **C**. **A** was generated as expected by treating diferrocenyl ketone [7] with methyl lithium, whereas **B** was not obtained in a similar fashion. Instead, a base-catalyzed intramolecular cyclization gives rise to a [3]ferrocenophane containing three ferrocene units. Herein we describe the synthesis and structure of this novel compound, **D**.

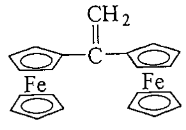

A

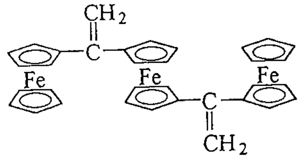

B

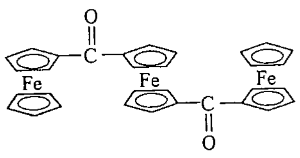

C

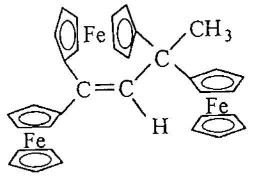

D

2. Results and discussion

Two compounds, diferrocenylketone [7] and 1,1-bis(ferrocenylcarbonyl)ferrocene **C** [8] were chosen as start-

---

* Corresponding author. Fax: + 886 2 29023209; e-mail: chem1009@fujens.fju.edu.tw

0022-328X/98/$19.00 © 1998 Elsevier Science S.A. All rights reserved.
PII S0022-328X(98)00561-0

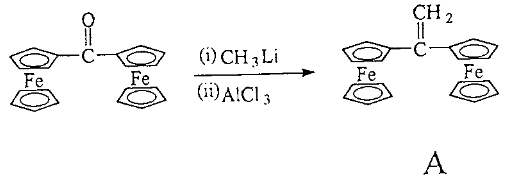

Scheme 1.

ing materials for the synthesis of **A** and **B**. The reduction of diferrocenylketone with methyl lithium and aluminum chloride in ether led to an orange–red substance which was characterized as 1,1-diferrocenylethene **A**. The synthesis is shown in Scheme 1.

Unlike its precursor diferrocenylketone and its analogue bis(methylene) compound [5], which show two-triplet and two-multiplet structure for the substituted Cp ring protons, **A** shows two-singlet. The reported proton NMR spectrum of [1,1]ferrocenophane [9], one singlet for bridged CH_2 protons, one multiplet each for ring α- and β- protons, suggests that there is no interaction between bridging methylene protons and α-protons, and that intramolecular interactions between H_α–H_α and H_β–H_β result in two sets of multiplet. In diferrocenylketone, the bridging sp^2 carbon stretches the two substituted Cp rings away from each other further than the bridging sp^3 carbon in [1,1]ferrocenophane, as indicated by the disappearance of H_α–H_α interaction, and the appearance of two-triplet structure due to H_α–H_β coupling. The vicinal coupling constant, 1.8 Hz for diferrocenylketone, decreases to indistinguishable as carbonyl group is replaced by ethylene group. The coupling constant equivalent for α- and β-protons in **A** may result from the decreasing electron-withdrawing capability of ethene group than carbonyl group.

After ascertaining that compound **A** was accessible by the reaction of CH_3Li and $AlCl_3$, an attempt was made to synthesize the compound **B** under the same condition. However, the main product this time is 1,3-diferrocenyl-3-methyl[3]ferrocenophan-1-ene **D** instead of **B**, as shown in Scheme 2.

In addition to two singlet at δ 1.76(methyl protons) and 6.66(methylene proton), the proton NMR spectrum of **D** shows seven distinguishable multiplet centered at δ 3.61, 3.93, 4.04, 4.06, 4.12, 4.29 and 4.41, respectively, with equal intensity, and some unresolved multiplet around the free Cp signal. The mass spectrum, on the other hand, is rather clean and simple with almost all peaks identified: 606 (M^+, 44%), 591 ($[M-CH_3]^+$, 47%), 421 ([M–Fc], 1%), 121 (C_5H_5Fe, 5%), 39 (?, 2%).

The structure of **D** is confirmed by X-ray crystallography. An ORTEP drawing with the atomic numbering scheme is shown in Fig. 1. Crystal data and details associated with structure refinement are summarized in Table 1. The selected bond lengths and angles are given in Table 2. C12A–C13A bond has a length of 1.327(2) Å which qualifies it as a carbon–carbon double bond. The dihedral angles between the ring planes in ferrocene units containing FE1A and FE3A are 4.48° and 1.64°, respectively. The obvious strain in the ferrocene unit containing FE2A is evidenced by 12.56° dihedral angle between the ring planes and comparison to 8.8° in [3]ferrocenophan-1-one [1]. This agrees to the fact that the most intense peak in the mass spectrum is $[M-CH_3]^+$ instead of the molecular ion, implicating a substantial stability gain by losing a methyl group.

In the absence of aluminum chloride, the reaction of **C** with methyl lithium in ether was carried out, and quenched with deoxygenated water. Mass studies of the reaction products suggest **E** to be the major intermedi-

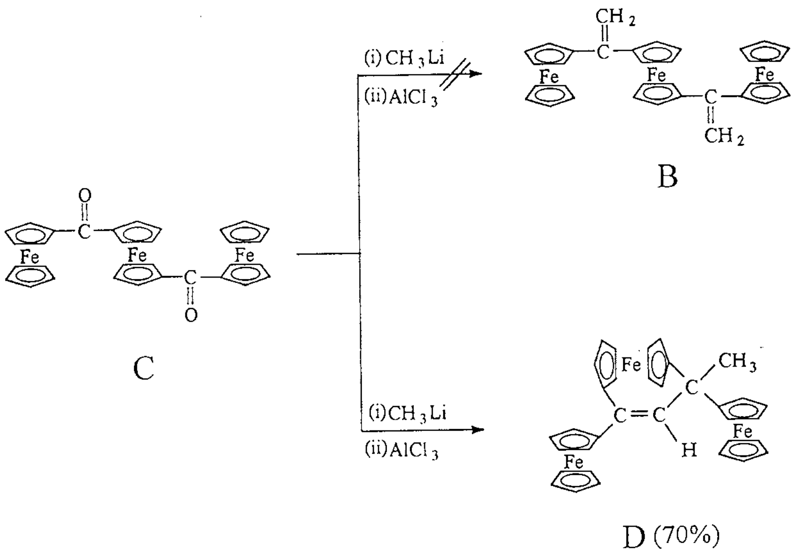

Scheme 2.

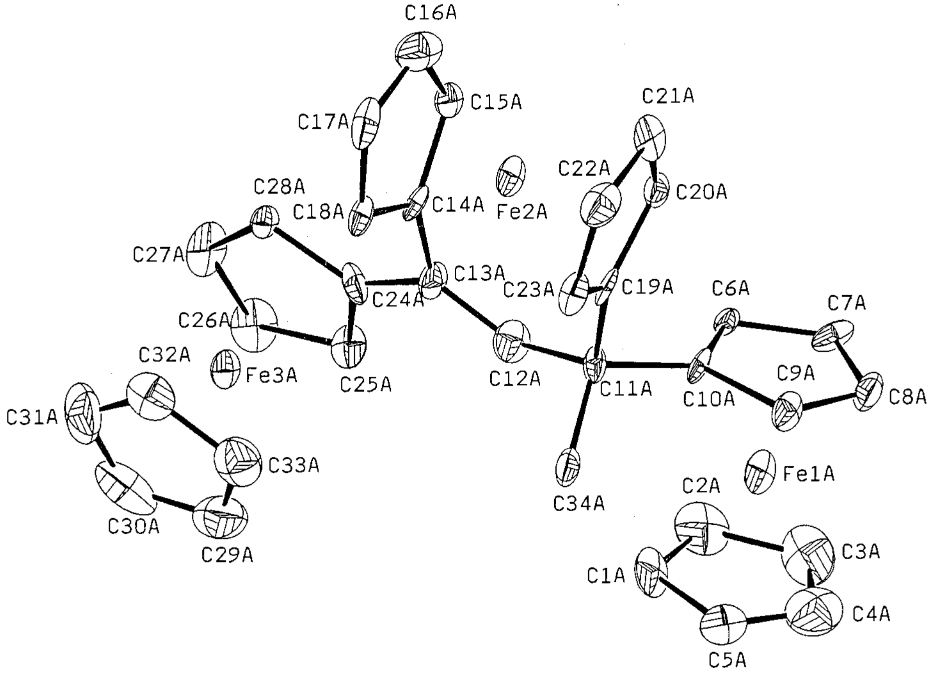

Fig. 1. An ORTEP drawing with the atomic number scheme.

ate, since the corresponding pinacol ($m/e = 642$) is the predominant species in the higher molecular weight range ($m/e > 400$). In addition to fragments from the pinacol ($m/e = 413$, 276), there exist also fragments ($m/e = 331$, 210) observed in the mass spectrum of **A**. Judging from the absence of molecular ion of **B** ($m/e = 606$), we believe these fragments result from partial self-condensation of the pinacol. All these observation can be accommodated for **D** in a mechanism, as in Scheme 3.

Table 1
Summary of crystallographic data for compound **D**, 1,3-diferrocenyl-3-methyl[3]ferrocenophan-1-ene

Empirical formula	$C_{34}H_{30}Fe_3$
Crystal size (mm)	$0.13 \times 0.40 \times 0.50$
Crystal system	Monoclinic
Space group	$P2_1/c$
a (Å)	15.580 (6)
b (Å)	9.512 (3)
c (A)	34.493 (9)
β (°)	98.20 (3)
V (Å^3)	5060 (3)
Z	8
Formula weight	606.15
d_{calcd} (g cm^{-1})	1.592
F(000)	2477
2θ range	26.14–47.06°
Scan type	$\theta/2\theta$
Scan speed (° min^{-1})	Variable; 2.06–8.24
Index ranges	$-16<h<16$, $0<k<10$, $0<l<36$
Reflecns collected	6364
Unique reflecns	6364
obsd reflecns ($I>2.06(I)$	3417
R_f^a (%)	7.3
R_w^b (%)	6.8
Goodness-of-fit	2.52

[a] $R_f = \Sigma\ \|F_0|-|F_c\|/\Sigma\ |F_0|$.
[b] $R_w = [\Sigma\ w(F_0|-|F_c)^2/\Sigma\ w|F_0|^2]^{1/2}$, $w^{-1} = \sigma^2|F_0|$.

In conclusion, the work presented in this paper has demonstrated a base-catalyzed intramolecular cyclization, and the potentiality of **C** as a building block for 'ferrocene clusters' [10]. Research to synthesize a compound like 2-oxa-1,1,3,3-tetraferrocenyl[3]ferrocenophane is currently under way.

3. Experimental

All synthesis and manipulations were carried out using standard Schlenk techniques. Solvents were dried according to published methods [11] by distillation under nitrogen from appropriate agents: benzene from sodium/benzophenone, dichloromethane from CaH_2. Chemicals were obtained from the following sources: $CDCl_3$ from MSD, Al_2O_3 from Fluka, and the rest from Aldrich. Melting points were determined on a Du Pont 910 Differential Scanning Calorimeter under nitrogen. ^{1}H-NMR spectra were obtained in $CDCl_3$ on a Bruker Aspect-3000 (300 MHz) spectrometer. The crystal structure analyses were performed with an Enraf–Nonius CAD-4 diffractometer with graphite-monochromated Cu K$_\alpha$ radiation.

Table 2
Selected bond lengths (Å) and angles (°) of compound **D**

Fe1A–C2A	2.034(14)	C16A–Fe2A–C23A	160.8(6)
Fe1A–C3A	2.036(16)	C16A–Fe2A–C23A	160.8(6)
Fe1A–C4A	2.021(16)	C17A–Fe2A–C18A	39.8(5)
Fe1A–C5A	2.061(13)	C17A–Fe2A–C20A	165.6(5)
Fe1A–C6A	2.052(12)	C17A–Fe2A–C19A	151.6(5)
Fe1A–C7A	2.046(13)	C17A–Fe2A–C21A	132.5(6)
Fe1A–C8A	2.020(13)	C17A–Fe2A–C23A	123.6(6)
Fe1A–C9A	2.049(13)	C18A–Fe2A–C19A	113.4(5)
Fe1A–C10A	2.071(13)	C18A–Fe2A–C20A	149.2(5)
Fe2A–C14A	1.984(12)	C18A–Fe2A–C21A	166.7(6)
Fe2A–C15A	2.020(13)	C18A–Fe2A–C21A	166.7(6)
Fe2A–C16A	2.070(15)	C18A–Fe2A–C22A	128.4(6)
Fe2A–C17A	2.066(14)	C19A–Fe2A–C20A	42.2(5)
Fe2A–C19A	1.991(13)	C19A–Fe2A–C21A	71.0(5)
Fe2A–C20A	2.002(14)	C19A–Fe2A–C23A	41.4(6)
Fe2A–C21A	2.027(13)	C20A–Fe2A–C22A	67.8(6)
Fe2A–C22A	2.011(15)	C20A–Fe2A–C23A	69.3(5)
Fe2A–C23A	2.003(13)	C21A–Fe2A–C22A	39.9(6)
Fe3A–C24A	2.050(13)	C21A–Fe2A–C23A	69.2(5)
Fe3A–C25A	2.049(14)	C22A–Fe2A–C23A	40.5(5)
Fe3A–C26A	2.014(15)	C10A–C11A–C12A	108.5(11)
Fe3A–C27A	2.024(14)	C10A–C11A–C19A	105.0(10)
Fe3A–C28A	2.039(12)	C10A–C11A–C34A	112.2(11)
Fe3A–C29A	2.000(14)	C12A–C11A–C19A	115.6(11)
Fe3A–C30A	2.039(15)	C12A–C11A–C19A	115.6(11)
Fe3A–C31A	2.067(15)	C12A–C11A–C34A	107.1(10)
Fe3A–C32A	2.028(15)	C11A–C12A–C13A	128.7(13)
Fe3A–C33A	2.059(16)	C12A–C13A–C14A	127.6(12)
C10A–C11A	1.532(19)	C12A–C13A–C24A	117.3(12)
C11A–C12A	1.562(19)	C14A–C13A–C24A	114.9(11)
C11A–C19A	1.555(18)	Fe2A–C14A–C15A	70.7(7)
C12A–C13A	1.327(20)	C13A–C14A–C18A	126.0(1i)
C13A–C24A	1.505(19)	C15A–C14A–C18A	107.1(11)
C14A–Fe2A–C15A	41.3(5)	Fe2A–C15A–C14A	68.0(7)
C14A–Fe2A–C16A	69.0(5)	Fe2A–C15A–C14A	68.0(7)
C14A–Fe2A–C17A	69.0(6)	Fe2A–C15A–C16A	71.6(8)
C14A–Fe2A–C18A	41.9(6)	Fe2A–C16A–C15A	67.8(8)
C14A–Fe2A–C19A	96.4(5)	Fe2A–C16A–C17A	69.9(8)
C14A–Fe2A–C20A	112.3(6)	Fe2A–C17A–C18A	69.2(8)
C14A–Fe2A–C21A	151.3(6)	Fe2A–C18A–C14A	66.8(7)
C14A–Fe2A–C22A	158.6(5)	Fe2A–C18A–C17A	70.9(8)
C14A–Fe2A–C23A	118.4(5)	Fe2A–C19A–C11A	126.0(9)
C15A–Fe2A–C16A	40.7(6)	Fe2A–C19A–C20A	69.3(7)
C15A–Fe2A–C17A	67.9(6)	Fe2A–C19A–C20A	69.3(7)
C15A–Fe2A–C18A	68.8(5)	Fe2A–C19A–C20A	69.3(7)
C15A–Fe2A–C19A	117.4(6)	Fe2A–C19A–C23A	69.8(8)
C15A–Fe2A–C20A	103.1(6)	C11A–C19A–C20A	125.6(12)
C15A–Fe2A–C21A	121.3(5)	C11A–C19A–C23A	128.3(12)
C15A–Fe2A–C22A	159.5(5)	Fe2A–C20A–C19A	68.5(7)
C15A–Fe2A–C23A	155.5(5)	Fe2A–C20A–C21A	70.2(S)
C16A–Fe2A–C17A	33.8(6)	Fe2A–C21A–C20A	68.2(7’
C16A–Fe2A–C18A	67.5(5)	Fe2A–C21A–C22A	69.4(8’
C16A–Fe2A–C19A	157.6(6)	Fe2A–C22A–C21A	70.7(8)
C16A–Fe2A–C20A	126.2(6)	C16A–Fe2A–C20A	126.2(6)
C16A–Fe2A–C21A	113.6(5)	Fe2A–C22A–C23A	69.4(8)
Fe2A–C23A–C19A	68.9(7)		
Fe2A–C23A–C22A	70.1(8)		

3.1. *Diferrocenylethene* ***A***

To a solution of diferrocenylketone [7] (300 mg, 0.754 mmol) in 50 ml of dry ether was added 5 ml (8 mmol) of 1.6 M solution of methyl lithium. The mixture was stirred at room temperature for 4 h under nitrogen. Then, an excess amount of aluminum chloride (2 g, 15 mmol) was added, and the resulting mixture was stirred for an additional 2 h. The reaction was quenched with deoxygenated water, the aqueous layer was separated, and the ether layer was chromatographed on silica gel with ether as the eluent. Recrystallization in ether–*n*-hexane solution gave orange–red solid. Yield: 200 mg (67%); m.p. 225°C (dec); Found: C, 66.34; H, 5.37; Fe, 28.29. $C_{22}H_{20}Fe_2$ calc.: C, 66.71; H, 5.09; Fe, 28.20. ^{1}H-NMR [$CDCl_3$] (ppm): δ 4.15 (s, 10H); 4.27 (s, 4H); 4.62 (s, 4H); 5.42 (s, 2H); mass spectrum, *m*/*e* (relative intensity) 396 (100), 331 (22), 210 (10), 121 (34).

3.2. *1,3-diferrocenyl-3-methyl[3]ferrocenophan-1-ene* ***B***

To a solution of 1,1-bis(ferrocenylcarbonyl)ferrocene **C** [8] (500 mg, 0.820 mmol) in 50 ml of dry ether was added 12 ml (19.2 mmol) of 1.6 M solution of methyl lithium. The mixture was stirred at room temperature for 4 h under nitrogen. Then, an excess amount of aluminum chloride (3 g, 22.5 mmol) was added, and the resulting mixture was stirred for an additional 2 h. After quenching the reaction with deoxygenated water, the aqueous was separated, and the organic layer was extracted with 150 ml chloroform. Chromatography was carried out on silica gel with benzene as the eluent. Crystallization done in benzene–*n*-hexane gave orange solid. Yield: 350 mg (70%); m.p. 218°C; Found: C, 67.39; H, 5.00; Fe, 27.61. $C_{34}H_{30}Fe_3$ calc.: C, 67.37; H, 4.99; Fe, 27.64.

4. Supplementary material available

Tables of full crystallographic data (one page), complete bond distance and angles (six pages), anisotropic thermal parameters (five pages), hydrogen atom positional parameters (22 pages) are available from the authors upon request.

Acknowledgements

We gratefully acknowledge support from the National Science Council. We also thank Dr. S.M. Peng and his staff for X-ray structure determination work.

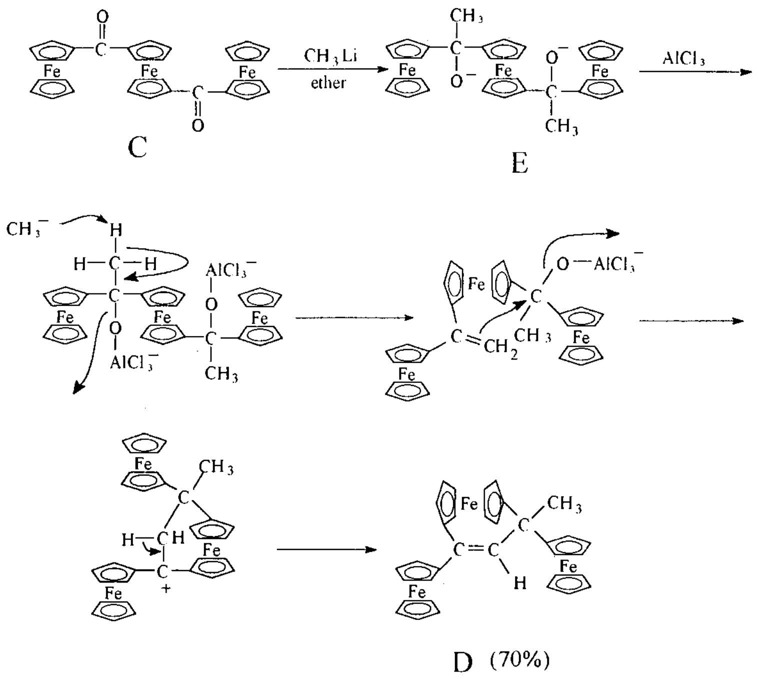

Scheme 3.

References

[1] W.E. Watts, Organomet. Chem. Rev. 2 (1967) 231, and references therein.

[2] (a) T.H. Barr, W.E. Watts, Tetrahedron 24 (1968) 3219. (b) T.H. Barr, W.E. Watts, Tetrahedron 24 (1968) 6111. (c) T.H. Barr, W.E. Watts, Tetrahedron 25 (1969) 861. (d) T.H. Barr, E.S. Bolton, H.L. Lentzner, W.E. Watts, Tetrahedron 25 (1969) 5245. (e) H.L. Lentzner, W.E. Watts, Tetrahedron 27 (1971) 4343. (f) H.Y. Lumbroso, C. Pigenet, H.L. Lentzner, W.E. Watts, Tetrahedron 28 (1972) 111. (g) H.L. Lentzner, W.E. Watts, Tetrahedron 28 (1972) 121. (h) T.D. Turbitt, W.E. Watts, Tetrahedron 28 (1972) 1227.

[3] (a) T.D. Turbitt, W.E. Watts, J. Organomet. Chem. 46 (1972) 109. (b) E.K. Heaney, S.R. Logan, W.E. Watts, J. Organomet. Chem. 150 (1978) 309.

[4] V.K. Kansal, W.E. Watts, U.T. Mueller-Westerhoff, A. Nazzle, J. Organomet. Chem. 243 (1983) 432, and references therein.

[5] U.T. Mueller-Westerhoff, Angew. Chem. Int. Ed. 25 (1986) 702, and references therein.

[6] U.T. Mueller-Westerhoff, G.F. Swiegers, Chem. Lett. (1994) 67, and references therein.

[7] D.C. O'Connor, D.O. Cowan, J. Organomet. Chem. 408 (1991) 219.

[8] T.H. Barr, H.L. Lentzner, W.E. Watts, Tetrahedron 25 (1969) 6001.

[9] A.L. Rheingold, U.T. Mueller-Westerhoff, G.F. Swiegers, T.J. Haas, Organometallics 11 (1992) 3411.

[10] T. Kinoschita, S. Tsuji, T. Otake, K. Takeuchi, J. Organomet. Chem. 458 (1993) 187.

[11] D.D. Perrin, W.L.F. Armarego, D.R. Perrin, Purification of Laboratory Chemicals, 2nd edn., Pergamon, Oxford, 1980.